JOURNAL OF GUIDANCE, CONTROL, AND DYNAMICS
Vol. 17, No. 6, November–December 1994

Controllability and Observability Measures for Craig-Bampton Substructure Representations

Michael J. Triller* and Daniel C. Kammer†
University of Wisconsin, Madison, Wisconsin 53706

Measures of controllability and observability are derived for a Craig-Bampton substructure representation for which fixed interface modes and constraint modes are computed relative to control actuator locations. The measures facilitate modal ordering and act as an index of dynamic completeness for modal truncation. Example problems are given to demonstrate that the controllable and observable reduced substructure models have a greater accuracy in predicting closed-loop pole locations, transfer functions, and actuation commands than conventional normal-mode models.

Introduction

DUE to the intimate relationship between the control and structural dynamics of proposed *large space structures* (LSS), there is a need for unification of the two disciplines. In general, the first step in the analysis of an LSS is the generation of a finite element representation. The resulting finite element model (FEM) is usually much too large for the efficient application of modern methods of control dynamics. In contrast, the structural dynamics community has had a great deal of success performing dynamic analysis with very large FEMs by using substructure representations. Over the past few years, researchers in the control dynamics community have sought to take advantage of this methodology in order to develop decentralized control strategies that reduce the computational complexity of controlling LSS.[1,2] However, the work to date has not taken full advantage of the substructure representations available in the context of control design.

This paper specifically addresses the advantages of using the Craig-Bampton (CB) substructure representation[3] in control system design. The CB representation is the basis of a well-known component mode synthesis technique developed to analyze linear structural dynamic problems of very high order. It is the most frequently used format in the aerospace industry for structural-load analysis. As a preliminary step toward future work in decentralized control, this investigation considers the complete LSS as a single CB representation. Instead of the usual interface degrees of freedom connecting to other substructures, there are now actuator locations that are constrained during the computation of fixed interface mode shapes used to describe the dynamics of the LSS internal to the actuator degrees of freedom.

The use of the CB representation in this fashion has been investigated to a small extent. Reference 4 demonstrated that fixed interface mode representations provide more accurate closed-loop pole locations and transfer functions for a smaller number of retained modes than the more conventional approach of using models based solely upon free-free modes. This is due to the static completeness of the CB mode set and the improved accuracy obtained in representing boundary conditions at actuator locations. However, in order for the CB substructure representation to be a truly useful tool in control system design, conditions for controllability and observability must be available. This investigation extends the work in Ref. 4 by deriving conditions and measures of controllability and observability corresponding to the CB state space.

Received March 17, 1993; revision received March 15, 1994; accepted for publication March 16, 1994.

*Graduate Student, Department of Engineering Mechanics and Astronautics. Student Member AIAA.

†Associate Professor, Department of Engineering Mechanics and Astronautics. Associate Fellow AIAA.

A vast amount of research has been devoted by the control dynamics community to the reduction of analytical models using measures of controllability and observability. In general, these measures indicate the importance of one state *relative* to another; however, they yield no absolute information on dynamic completeness. On the other hand, the structural dynamics community has developed an absolute measure of dynamic importance based upon the contribution of a mode shape to dynamic loading. This measure, called *effective modal mass,*[5] has been used to reduce models for subsequent structural-load analysis and to select important target modes for modal surveys. This paper shows that a generalization of this measure, called *effective interface mass,*[6] is related to controllability and observability measures for the CB state space. It will be shown that effective interface mass can be used not only as a measure of dynamic completeness, but also as an absolute measure of controllability and, in the case of collocated sensing, an absolute measure of observability. Use of the CB representation thus unifies the measures of controllability (observability) and dynamic importance.

Craig-Bampton Substructure Representation

An actuator configuration is assumed to have been chosen using an established placement technique.[7] The n physical degrees of freedom (dof) of the FEM are partitioned into two complementary sets: a with n_a dof and o with n_o dof where the a set includes all actuator degrees of freedom. This results in an equation of motion for the free-free undamped structure of the form

$$\begin{bmatrix} M_{aa} & M_{ao} \\ M_{oa} & M_{oo} \end{bmatrix} \begin{Bmatrix} \ddot{x}_a \\ \ddot{x}_o \end{Bmatrix} + \begin{bmatrix} K_{aa} & K_{ao} \\ K_{oa} & K_{oo} \end{bmatrix} \begin{Bmatrix} x_a \\ x_o \end{Bmatrix} = \begin{Bmatrix} F_a \\ 0 \end{Bmatrix} \tag{1}$$

where it has been assumed that loads are applied only at actuator locations. Considering the lower partition of the static portion of Eq. (1) and solving for the displacements of the o set in terms of the displacements of the actuator set, we obtain the relationship

$$x_o = -K_{oo}^{-1} K_{oa} x_a = \Psi x_a \tag{2}$$

Constraining the actuator displacements to zero, a set of *fixed actuator modes* Φ can be obtained by solving the corresponding eigenproblem. The results of Eq. (2) and the fixed actuator modes can be combined into a set of displacement vectors that can be used to generate a transformation from the original FEM configuration space of Eq. (1) to the CB coordinate space

$$x = \begin{bmatrix} I_a & 0 \\ \Psi & \Phi \end{bmatrix} \begin{Bmatrix} x_a \\ q \end{Bmatrix} = T x_{\mathrm{CB}} \tag{3}$$

where I_a is an $n_a \times n_a$ identity matrix as indicated by the subscripts and 0 is an $n_a \times n_o$ block zero matrix. The first partition of columns in Eq. (3) are static shapes called *control constraint modes*. Each of the columns represents the static deformation of the structure when one of the actuator locations is given a unit displacement whereas

all other actuator locations are fixed. The second column partition contains the fixed actuator modes that describe the system dynamics relative to the actuators. It has been assumed that the fixed actuator modes are normalized with respect to the mass matrix partition M_{oo}. The coordinate space of the CB representation contains the physical displacements of the actuators x_a and the modal displacements of the the fixed actuator modes q. The mass and stiffness matrices of the FEM representation are transformed using Eq. (3), resulting in the equation of motion

$$\begin{bmatrix} M_{aa} + \Psi^T M_{oa} + M_{ao}\Psi + \Psi^T M_{oo}\Psi & M_{ao}\Phi + \Psi^T M_{oo}\Phi \\ \Phi^T M_{oa} + \Phi^T M_{oo}\Psi & I_o \end{bmatrix} \times \begin{Bmatrix} \ddot{x}_a \\ \ddot{q} \end{Bmatrix} + \begin{bmatrix} K_{aa} + K_{ao}\Psi & 0 \\ 0 & \Lambda \end{bmatrix} \begin{Bmatrix} x_a \\ q \end{Bmatrix} = \begin{bmatrix} I_a \\ 0 \end{bmatrix} u \tag{4}$$

or equivalently

$$\begin{bmatrix} \mathcal{M}_{aa} & \mathcal{M}_{ao} \\ \mathcal{M}_{oa} & I_o \end{bmatrix} \begin{Bmatrix} \ddot{x}_a \\ \ddot{q} \end{Bmatrix} + \begin{bmatrix} \mathcal{K}_{aa} & 0 \\ 0 & \Lambda \end{bmatrix} \begin{Bmatrix} x_a \\ q \end{Bmatrix} = \begin{bmatrix} I_a \\ 0 \end{bmatrix} u \tag{5}$$

where $\Lambda = \text{diag}\{\lambda_1, \ldots, \lambda_Q\}$ is a diagonal matrix of the n_o fixed actuator mode eigenvalues. There are Q distinct eigenvalues, each with multiplicity n_q, so that $n_o = n_1 + n_2 + \cdots + n_Q$.

Effective Interface Mass

The effective interface mass measure is developed by considering the lower partition of Eq. (4), which governs the response of the fixed actuator modal coordinates

$$\ddot{q} + \Lambda q = -\left(\Phi^T M_{oo}\Psi + \Phi^T M_{oa}\right)\ddot{x}_a \triangleq P\ddot{x}_a \tag{6}$$

The $n_o \times n_a$ matrix P is called the *modal participation factor matrix*.[5] The jth entry in the ith row P_i represents the extent to which fixed actuator mode i is excited by a unit acceleration of actuator degree of freedom j. The upper partition of Eq. (4) governs motion of the actuator degrees of freedom, which may be expressed as

$$M_s\ddot{x}_a + K_s x_a + \left(\Psi^T M_{oo}\Phi + M_{ao}\Phi\right)\ddot{q} = F_a \tag{7}$$

where M_s and K_s are the static reductions of the mass and stiffness matrices to the a set, $K_s = K_{aa} + K_{ao}\Psi$, $M_s = M_{aa} + M_{ao}\Psi + \Psi^T M_{oa} + \Psi^T M_{oo}\Psi$. If the actuator degrees of freedom are fixed, the constraint forces are given by

$$F_a = \left[\Psi^T M_{oo}\Phi + M_{ao}\Phi\right]\ddot{q} = -P^T\ddot{q} \tag{8}$$

Assuming harmonic motion of the fixed actuator modes and that they respond in phase, a conservative estimate of the total constraint force may be expressed as

$$F_a = \mathcal{M}\lambda^{1/2}V \tag{9}$$

where $\mathcal{M} = P^T P$ and V is a convolution integral.

The accuracy of the actuator loads predicted by a reduced analytical representation, where $n_k < n_o$ fixed actuator modes are retained, can be measured by comparing the retained matrix $\mathcal{M}^r$ relative to the complete matrix $\mathcal{M}$ using an appropriate matrix norm. The matrix $\mathcal{M}$ will be referred to as the *reduced interior mass matrix*, which, using the definition of P, can be written as

$$\mathcal{M} = \Psi^T M_{oa} + M_{ao}\Psi + \Psi^T M_{oo}\Psi + M_{ao}M_{oo}^{-1}M_{oa} \tag{10}$$

This expression can be computed independent of any eigensolution; it depends only on the system mass and stiffness matrix partitions. Therefore, $\mathcal{M}$ can be used as an absolute reference with respect to which the dynamic importance of each mode shape can be computed.

In order to compute the effective interface mass measure, the term-by-term square of the modal participation factor matrix is formed,

$$\Sigma = P^{\wedge 2} = \left[-\left(\Phi^T M_{oo}\Psi + \Phi^T M_{oa}\right)\right]^{\wedge 2} \tag{11}$$

where $[\bullet]^{\wedge 2}$ indicates the term-by-term square. Each column of Σ sums to the corresponding diagonal term in the reduced interior mass matrix $\mathcal{M}$. Matrices $\mathcal{M}$ and Σ are then partitioned according to translational and rotational degrees of freedom within the a set,

$$\mathcal{M} = \begin{bmatrix} \mathcal{M}_T & \mathcal{M}_{TR} \\ \mathcal{M}_{RT} & \mathcal{M}_R \end{bmatrix}, \qquad \Sigma = [\,\Sigma_T \quad \Sigma_R\,] \tag{12}$$

in which subscripts T and R denote translational and rotational partitions, respectively.

The columns of Σ_T and Σ_R must be properly weighted to account for the importance of one actuator degree of freedom relative to another by separately adding their columns together and dividing by the trace of $\mathcal{M}_T$ and $\mathcal{M}_R$, respectively, producing the $n_o \times 2$ matrix

$$\Sigma_N = [\,\Sigma_T \quad \Sigma_R\,] \begin{bmatrix} 1_T & 0_T \\ 0_R & 1_R \end{bmatrix} \begin{bmatrix} \frac{1}{\text{tr}(\mathcal{M}_T)} & 0 \\ 0 & \frac{1}{\text{tr}(\mathcal{M}_R)} \end{bmatrix} \tag{13}$$

in which 1_T denotes a column vector of 1's and 0_T a null vector both of dimension equal to the number of translational actuator degrees of freedom. Analogous definitions apply to terms with the subscript R. The ith entry in the first column of Σ_N is the fractional contribution of the ith fixed actuator mode to the trace of the translational actuator portion of the reduced interior mass matrix, whereas the corresponding term in the second column gives the fractional contribution to the trace for the rotational partition. The columns of Σ_N are dimensionless and can therefore be averaged to produce the normalized effective interface mass vector

$$\sigma = \tfrac{1}{2}[\,\Sigma_{NT} \quad \Sigma_{NR}\,] \begin{Bmatrix} 1 \\ 1 \end{Bmatrix} \tag{14}$$

in which the ith term represents the fractional contribution of the ith fixed actuator mode to the weighted trace of the reduced interior mass matrix. Further details can be found in Ref. 6.

Controllability

A measure of controllability is now derived for the CB representation discussed above. The derivations presented here are in the spirit of those presented by Hughes and Skelton[8,9], Ohkami and Likins,[10] and Likins et al.[11] First consider a configuration where the actuators are placed to fully constrain rigid-body motion, but in a statically indeterminate manner. For this case, the stiffness partition $\mathcal{K}_{oo}$ is nonsingular and the control constraint modes can be calculated using Eq. (2).

The CB representation in Eq. (5) can be expressed in first-order form as

$$\dot{z} = Az + Bu \tag{15}$$

where the state vector is

$$z = \begin{Bmatrix} x_a \\ q \\ \dot{x}_a \\ \dot{q} \end{Bmatrix} \in \mathbb{R}^{2n \times 2n}$$

and the system matrices are given by

$$A = \begin{bmatrix} 0 & 0 & I & 0 \\ 0 & 0 & 0 & I \\ -\mathcal{M}\mathcal{K}_{aa} & \mathcal{M}\mathcal{M}_{ao}\Lambda & 0 & 0 \\ \mathcal{M}_{oa}\mathcal{M}\mathcal{K}_{aa} & -(\mathcal{M}_{oa}\mathcal{M}\mathcal{M}_{oa} + I_{oo})\Lambda & 0 & 0 \end{bmatrix},$$

$$B = \begin{bmatrix} 0 \\ 0 \\ \mathcal{M} \\ -\mathcal{M}_{oa}\mathcal{M} \end{bmatrix}$$

in which $\mathcal{M} \triangleq (I_{oo} - \mathcal{M}_{aa}^{-1}\mathcal{M}_{ao}\mathcal{M}_{oa})^{-1}\mathcal{M}_{aa}^{-1}$. The condition for controllability of the above system is given by the following theorem.[12]

Theorem 1. For the linear time-invariant (LTI) system of Eq. (15), the pair (A, B) is controllable if and only if

$$\rho[\,B \quad AB \quad A^2B \quad \cdots \quad A^{2n-1}B\,] = 2n \tag{16}$$

where ρ denotes the rank operator and U is the controllability test matrix.

Invariance of controllability to the state feedback $u = -Gz$ is established by the following theorem.[13]

Theorem 2. The pair (A, B) is controllable if and only if the pair $(\tilde{A}, B)$ is controllable where $A = \tilde{A} + BG$.

This theorem can be used to simplify the rank test for controllability. For the choice

$$\tilde{A} = \begin{bmatrix} 0 & 0 & I & 0 \\ 0 & 0 & 0 & I \\ 0 & 0 & 0 & 0 \\ 0 & -\Lambda & 0 & 0 \end{bmatrix} \tag{17}$$

the matrix $G = [-\mathcal{K}_{aa}\ \mathcal{M}_{ao}\Lambda\ 0\ 0]$ satisfies $A = \tilde{A} + BG$. Since Theorem 2 is necessary and sufficient, (A, B) is controllable if and only if $(\tilde{A}, B)$ is controllable. So conditions for the controllability of (A, B) may be established by testing the controllability matrix of the greatly simplified pair $(\tilde{A}, B)$.

The resulting controllability matrix has the form

$$U = \begin{bmatrix} 0 & \bar{B} & \cdots & 0 & (-D)^{n-1}\bar{B} \\ \bar{B} & 0 & \cdots & (-D)^{n-1}\bar{B} & 0 \end{bmatrix} \tag{18}$$

where

$$\bar{B} = \begin{bmatrix} \mathcal{M} \\ -\mathcal{M}_{oa}\mathcal{M} \end{bmatrix}, \qquad \tilde{A} = \begin{bmatrix} 0 & I \\ -D & 0 \end{bmatrix}, \qquad D = \begin{bmatrix} 0 & 0 \\ 0 & \Lambda \end{bmatrix} \tag{19}$$

Noting that each block row contributes equally to the row rank of U, the rank test may be equivalently expressed as

$$\rho(\tilde{U}) = \rho[\,\bar{B}\ D\bar{B}\ D^2\bar{B} \cdots D^{n-1}\bar{B}\,] = n \tag{20}$$

The Jordan form controllability theorem[12] can be stated in the following manner.

Theorem 3. For the LTI system of Eq. (15) with $A \in \mathbb{R}^{n\times n}$ there exists a diagonal matrix with nondistinct elements $A = \text{diag}\{\lambda_1(\text{mult. } n_1), \ldots, \lambda_Q \text{ (mult. } n_Q)\}$, where $\sum_{i=1}^{Q} n_i = n$ and $B \in \mathbb{R}^{n\times a}$, partitioned as

$$B \triangleq \begin{bmatrix} B_1 \\ \vdots \\ B_Q \end{bmatrix} \begin{matrix} n_1 \text{ rows} \\ \\ n_Q \text{ rows} \end{matrix} \tag{21}$$

$$\rho[\,B\ AB \cdots A^{n-1}B\,] = n \quad \text{iff} \quad \rho[B_q] = n_q \quad (q = 1, \ldots, Q)$$

Noting that, in Eq. (20), D is diagonal, the Jordan form controllability theorem may be applied directly by properly partitioning $\bar{B}$ according to the Jordan form of D as

$$\bar{B} = \begin{bmatrix} \bar{B}_0 \\ \bar{B}_1 \\ \vdots \\ \bar{B}_Q \end{bmatrix} = \begin{bmatrix} \mathcal{M} \\ -(\mathcal{M}_{oa}\mathcal{M})_1 \\ \vdots \\ -(\mathcal{M}_{oa}\mathcal{M})_Q \end{bmatrix} \begin{matrix} n_0 = N_a \text{ rows} \\ n_1 \text{ rows} \\ \vdots \\ n_Q \text{ rows} \end{matrix} \tag{22}$$

where $(\cdot)_i$ refers to the n_i rows corresponding to Jordan block $D_i = \text{diag}(\lambda_i)$.

By Theorem 3, the pair $(\tilde{A}, B)$ is controllable if and only if

$$\rho(\bar{B}_0) = \rho(\mathcal{M}) = n_a \tag{23}$$

$$\rho(\bar{B}_q) = \rho[-(\mathcal{M}_{oa}\mathcal{M})_q] = n_q, \qquad q = 1, \ldots, Q \tag{24}$$

Since $\mathcal{M}$ is positive definite, the condition given by Eq. (23) is always satisfied. This implies that the control constraint modes are controllable by definition. Retaining the control constraint modes also preserves a statically complete mode set in the truncated model. The controllability condition is then determined solely by Eq. (24). Noting that $(\mathcal{M}_{oa}\mathcal{M})_q \equiv (\mathcal{M}_{oa})_q\mathcal{M}$ and that multiplication by a nonsingular matrix does not affect rank, the controllability rank condition may be expressed as

$$\rho[-(\mathcal{M}_{oa})_q] = \rho\left[-\left(\Phi^T M_{oo}\Psi + \Phi^T M_{oa}\right)_q\right] = n_q \tag{25}$$

where $q = 1, \ldots, Q$. Recalling the definition of the modal participation factor from Eq. (6), it is apparent that $(\tilde{A}, B)$ is controllable if the rows of the modal participation factor matrix corresponding to each Jordan block of D are linearly independent. The following result is obtained by application of Theorem 2.

Result 1. The matrix pair (A, B) of Eq. (15) is controllable if and only if

$$\rho(P_q) = n_q, \qquad q = 1, \ldots, Q \tag{26}$$

where n_q is the multiplicity of eigenvalue λ_q corresponding to Jordan block D_q $(q = 1, \ldots, Q)$ of Eq. (19) and P_q is the corresponding row partition of the modal participation factor matrix.

This result is a controllability condition. Recalling the discussion of effective interface mass, the following measure of controllability is proposed.

Proposition 1. Whenever Eq. (26) is satisfied, the controllability measure of the ith fixed actuator mode of the system in Eq. (15) is given by σ_i, the ith element of the $n_o \times 1$ effective interface mass vector given in Eq. (14).

Therefore, whenever Eq. (26) is satisfied, Eq. (14) serves as both a measure of controllability and a measure of dynamic importance. The fixed actuator modes may be ranked and the subset that contributes the desired amount to the completeness index is retained in the reduced model. The desired value is typically a percentage of the total reduced interior mass, such as 90 or 95%. When all the eigenvalues are distinct, as is often the case, Eq. (14) may be used without consideration of Eq. (26).

Although controllability is invariant to state feedback, controllability measures are not. The above discussion establishes a relationship between controllability and effective interface mass. The proposed measure is not the usual measure of controllability based upon condition number (singular values) of the controllability test matrix, but is a measure in the sense discussed in the previous section.

Now consider the special case where the actuators are placed to fully constrain rigid-body motion, but in a statically determinate manner. For this case it can be shown that $\mathcal{K}_{aa} = K_{aa} + K_{ao}\Psi = 0$. The stiffness partition $\mathcal{K}_{oo}$ is nonsingular and Eq. (2) can still be used to calculate the control constraint modes. The process discussed above can be repeated with this simplification and again leads to Result 1 and Proposition 1. Note that the control constraint modes Ψ are simply the rigid-body modes Φ_r of the LSS with a unit displacement at the actuator degrees of freedom. If the mass matrix is lumped, the resulting reduced interior mass matrix can be expressed as

$$\mathcal{M} = P^T P = \left[\Phi^T M_{oo}\Phi_r\right]^T\left[\Phi^T M_{oo}\Phi_r\right] = \Phi_r^T M_{oo}\Phi_r \tag{27}$$

which is the o-set rigid-body mass matrix. In this case, the ith element of σ represents the fractional contribution of the ith fixed interface mode to the weighted trace of the reduced rigid-body mass matrix.

For actuator configurations that do not fully constrain rigid-body motion, special consideration must be made. The stiffness matrix partition $\mathcal{K}_{oo}$ is now singular, and Eq. (2) can no longer be used to calculate the control constraint modes. This case corresponds to situations where a rigid-body direction of the LSS is deemed to be dynamically unimportant and is not controlled. To compute the control constraint modes in this case, the elastic flexibility matrix G_{oo}^e must be generated by projecting a fully constrained flexibility matrix onto the elastic mode space using an oblique projector. The control constraint modes are then given by $\Psi = -G_{oo}^e K_{oa}$. Details

of this computation can be found in Ref. 14. Once the constraint modes are obtained, it is easily shown that the previous results apply. Thus, conditions for controllability of CB representations may be determined for any general actuator configuration, including those with unconstrained rigid-body motion.

Observability

The dual problem of observability for the CB representation is investigated by considering the first-order system (15) with the separated output equation

$$y = Cz, \qquad C = \begin{bmatrix} P & 0 \\ 0 & Q \end{bmatrix} \tag{28}$$

where $P \in \mathbb{R}^{n_p \times n}$, $Q \in \mathbb{R}^{n_v \times n}$, and n_p and n_v are the number of position and velocity sensors, respectively. The observability condition can be derived in general, but this paper will concentrate on the special, but important, case of collocated sensors and actuators where a simple result can be obtained. The case where sensors are placed in addition to the collocated set will also be discussed.

The observability condition is given in the following theorem.[12]

Theorem 4. For the LTI system of Eq. (15) with output equation (28), the pair (A, C) is observable if and only if

$$\rho[\, C^T \quad A^T C^T \quad \cdots \quad (A^T)^{2n-1} C^T \,] = 2n \tag{29}$$

where ρ denotes the rank operator and Θ is the observability test matrix.

When one position sensor is collocated with each actuator, the following theorem[13] may be effectively exploited to simplify the observability test using output position feedback.

Theorem 5. The closed-loop matrix pair $(\tilde{A}, C)$ with $\tilde{A} = A - BGC$ is observable if and only if the open-loop pair (A, C) is observable.

Under the output feedback $u = -Gy = -GCz$, where

$$P = \begin{bmatrix} I_a & 0 \\ 0 & 0 \end{bmatrix}, \qquad Q = 0 \tag{30}$$

the gain

$$G = [\, \mathcal{K}_{aa} \quad 0 \quad 0 \quad 0 \,] \tag{31}$$

results in the closed-loop system matrix

$$\tilde{A} = \begin{bmatrix} 0 & I \\ -D_{cl} & 0 \end{bmatrix}, \qquad D_{cl} = \begin{bmatrix} 0 & D_{aq} \\ 0 & D_{qq} \end{bmatrix} \tag{32}$$

in which $D_{aq} = -M_{aa}^{-1} \Psi^T M_{oo} \Phi \Lambda$ and $D_{qq} = (\Phi^T M_{oo} \Psi M_{aa}^{-1} \Psi^T M_{oo} \Phi + I_o)\Lambda$.

The observability of (A, C) may then be investigated by applying Theorem 4 to the simplified pair $(\tilde{A}, C)$. The resulting rank test can be shown to be equivalent to the test

$$\rho(\bar{\Theta}) = \rho \begin{bmatrix} I_a & 0 & 0 & \cdots & 0 \\ 0 & D_{aq}^T & D_{qq}^T D_{aq}^T & \cdots & (D_{qq}^T)^{n-2} D_{aq}^T \end{bmatrix} = n \tag{33}$$

This observability condition then reduces to

$$\rho(\hat{\Theta}) = \rho\big[\, \mathcal{M}_{ao}^T \mathcal{M}^T \quad \Lambda \mathcal{M}_{ao}^T \mathcal{M}^T \quad \cdots \quad \Lambda^{n_o - 1} \mathcal{M}_{ao}^T \mathcal{M}^T \,\big] = n_o \tag{34}$$

which is well suited for the Hautus matrix test[12] given in Theorem 6.

Theorem 6. The rank of the matrix $\hat{\Theta}$ of Eq. (34) is n_o if and only if

$$\rho\big[\lambda I - \Lambda \;\vdots\; \mathcal{M}_{ao}^T \mathcal{M}^T\big] = n_o \qquad \forall \lambda \in \mathbb{C} \tag{35}$$

which is satisfied if and only if

$$\rho\big[\big(\mathcal{M}_{ao}^T \mathcal{M}^T\big)_q\big] = n_q, \qquad q = 1, \ldots, Q \tag{36}$$

where $(\mathcal{M}_{ao}^T \mathcal{M}^T)_q$ are the rows of $\mathcal{M}_{ao}^T \mathcal{M}^T$ corresponding to Jordan block D_q of Λ.

With this theorem, recalling the results of the controllability section, the following result is obtained.

Result 2. The matrix pair (A, C) is observable if and only if

$$\rho(P_q) = n_q, \qquad q = 1, \ldots, Q \tag{37}$$

where n_q is the multiplicity of eigenvalue λ_q corresponding to Jordan block D_q $(q = 1, \ldots, Q)$ and P_q is the corresponding row partition of the modal participation factor matrix.

An associated measure of observability can now be proposed.

Proposition 2. Whenever Eq. (37) is satisfied, the observability measure of the ith fixed actuator mode of the system in Eq. (15) is given by σ_i, the ith element of the $n_o \times 1$ effective interface mass vector given in Eq. (14).

The observability of the control constraint modes is guaranteed by the I_a partition of Eq. (33) as long as $n_a \geq n_r$ where n_r is the number of rigid-body directions. This requires at least one spatially independent sensor for each rigid-body direction, as expected.

When collocated rate sensors are used, output feedback does not lend itself to simplification of the dynamical matrix. Using the output influence matrix from Eq. (28), where now

$$Q = \begin{bmatrix} I_a & 0 \\ 0 & 0 \end{bmatrix}, \qquad P = 0 \tag{38}$$

the following two results can be obtained from Theorem 4 by examination of the observability test matrix (29).

(a) If $\rho(\mathcal{K}_{aa}) < n_a$, as would be the case if rigid-body modes are present, the system will not be observable with velocity sensors alone, which is consistent with theory.[15]

(b) If $\rho(\mathcal{K}_{aa}) \geq n_a$, i.e., no rigid-body modes, the system may be shown to be observable iff $\rho(P_q) = n_q$, $q = 1, \ldots, Q$, which is identical to the condition found for collocated position sensing.

Analogous to the controllability case, the observability condition is invariant to output feedback but the observability measures are not. The simplifications used to obtain the measures establish a relationship between observability and the effective mass measures discussed previously.

It is also of interest to examine cases where there are additional sensors complimenting the collocated set. Consider collocated position sensors with n_e additional noncollocated position sensors as an example (similar results may be obtained for collocated position plus rate sensors, etc.). The corresponding output influence matrix is given by

$$C = \begin{bmatrix} I_a & 0 & 0 & 0 \\ C_o \Psi & C_o \Phi & 0 & 0 \end{bmatrix}, \qquad C_o \in \mathbb{R}^{n_e \times n_o} \tag{39}$$

Using arguments similar to those in previous sections, the following result may be obtained.

Result 3. With C given by Eq. (39), the matrix pair (A, C) is observable if and only if $\rho(L_q) = n_q (q = 1, \ldots, Q)$, where L_q are row partitions of the matrix $L = [\Phi^T C_o^T \quad \Lambda P \mathcal{M}^T]$ corresponding to Jordan block q of Λ.

Unlike the previous collocated case, the dependence on the fixed actuator modes is apparent. Thus, any measure of observability with additional noncollocated sensors will likely not be absolute. This does not affect the observability condition, but does affect the observability measure. In this case, it is proposed that ranking of the fixed interface modes can be based solely upon the controllability measure. It is sufficient to note that the observability condition is met and that the corresponding observability measure meets or exceeds the controllability measure for each fixed actuator mode.

Application to Model Reduction

As an application of the above measures, consider model reduction for a simple uniform, free-free beam, as illustrated in Fig. 1. The model has a transverse dof at each grid and a single rotational dof at grid 11, producing 2 rigid-body modes and 20 flexible modes. The beam is controlled using 3 actuators: force actuators at grids

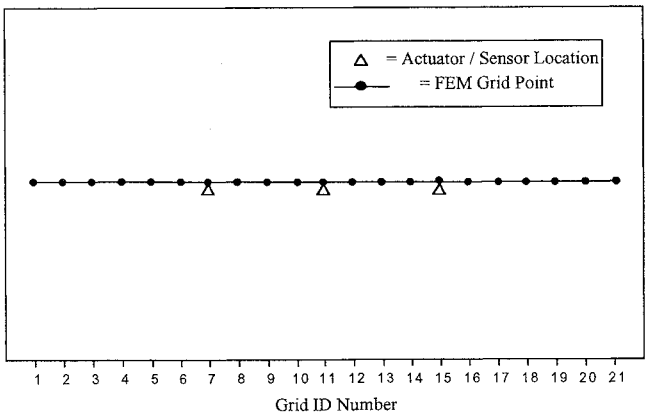

Fig. 1 Uniform free-free beam FEM.

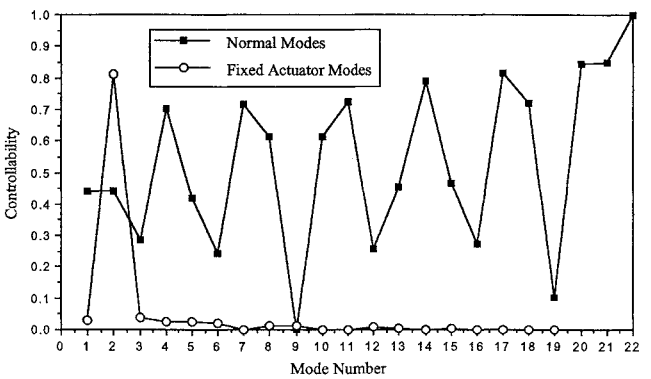

Fig. 2 Unsorted controllability.

7 and 15, and a torque device at grid 11. Sensors are collocated with the actuators. The analysis proceeds by constraining the beam at the actuator degrees of freedom and solving the corresponding eigenproblem resulting in 19 fixed actuator mode shapes.

The fixed actuator controllability (observability) measures σ_i are computed using Eq. (14) and are plotted in Fig. 2. Fixed actuator mode 2 is seen to contribute 81.1% to the weighted trace of the reduced interior mass for this actuator configuration. All other fixed actuator modes contribute less than 5%. Figure 3 illustrates the vector σ sorted in descending order. This plot can be used to quickly reduce the number of fixed actuator modes from the original 19 down to the four top contributors (2, 3, 1, and 5) to the weighted trace of the reduced interior mass matrix (RIM), retaining more than 90% of the total. The reduced CB model for the beam will contain these four fixed actuator modes and the three control constraint modes.

In contrast to the approach presented in this paper, the common practice is to transform the physical equations of motion (1) to modal coordinates. Controllability (observability) measures for the qth mode can be easily computed using the expression developed by Hughes and Skelton[8] given by $\mathcal{C}_q = |\tilde{B}_q^T \tilde{B}_q|^{1/2n_q}$, where $\tilde{B}_q$ is the row partition of $\Phi_p^T B_p$ corresponding to eigenvalue λ_q with multiplicity n_q. The matrix Φ_p is the modal matrix for the system in Eq. (1), and B_p is the corresponding input influence matrix.

These measures were computed and normalized for all 22 modes of the beam example, resulting in the controllability plot shown in Fig. 2. Figure 3 illustrates the controllability vector after it has been sorted in descending order for comparison with the effective interface mass measure. The plot of the normal-mode controllability measure offers virtually no information as to where the analyst should truncate the model. Moreover, once a truncation decision has been made, this measure offers no information as to the dynamic integrity of the reduced representation. It only provides a measure of the controllability of one mode relative to another. In contrast, if 90 or 95% of the weighted trace of the reduced interior mass is retained in the reduced CB representation, the corresponding closed-loop model will accurately predict the dynamically important closed-loop pole locations and response of the full-order system.

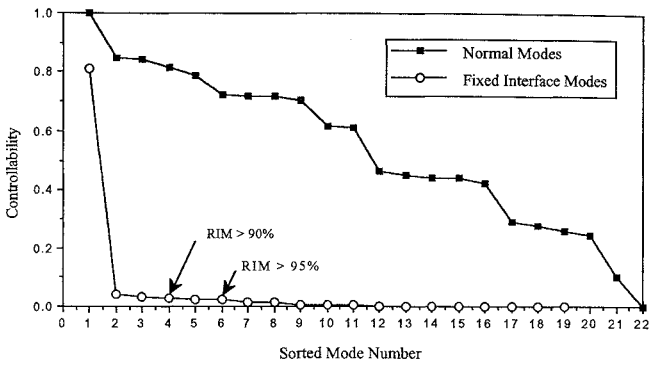

Fig. 3 Sorted controllability.

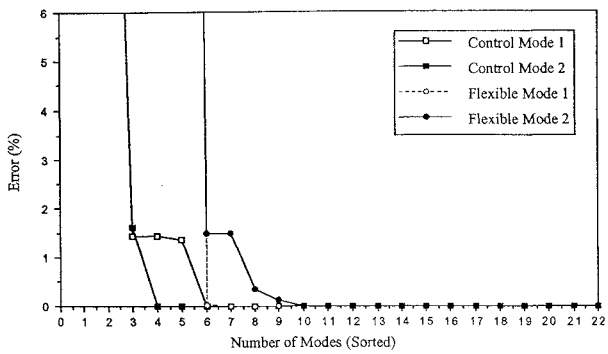

Fig. 4 Error in Craig-Bampton representation closed-loop s-plane pole location with varying number of modes.

This can be seen by comparing the closed-loop pole location errors computed using both the reduced CB and reduced normal-mode representations. A proportional-plus-derivative controller is developed using a virtual passive design approach[16] for the full-order model. The objectives are to place both the control modes (controlled rigid-body modes) at frequencies above 1 Hz with damping factors of 0.707 and provide as much damping as possible in the first and second flexible modes. The design using the full model results in closed-loop control mode frequencies of 1.22 and 1.25 Hz with damping factors of 0.73 and 0.49, respectively. The first and second flexible modes have closed-loop frequencies of 5.0 and 14.80 Hz with damping factors of 0.05 and 0.27, respectively. By considering the controller design implemented on the full model as "exact," closed-loop s-plane pole location errors due to modal truncation may be assessed. The relative error is defined as[4]

$$\text{Percent error} = \frac{|s - s'|}{|s|} \times 100\% \tag{40}$$

which represents a normalized distance from the exact location s to the approximate location s'.

Figure 4 shows the errors in the four target modes as fixed interface modes are added to the closed-loop CB representation in the order determined by their controllability measure. The first three modes are the constraint modes, which must be retained. The errors are seen to drop dramatically as fixed interface modes are added. When four fixed interface modes have been added, more than 90% of the dynamic completeness index is retained and errors are substantially less than 0.1% except in the second flexible mode, which is less than 1.5%. If six fixed interface modes are added, more than 95% of the dynamic completeness index is retained and all target mode errors are less than 1/100th of 1%. Figure 5 shows the errors in the first four target modes as normal modes are added to the closed-loop representation. The normal-mode controllability measure discussed above is not directly related to dynamic importance so it would make little sense to add modes in order of their controllability measure. Thus, modes are included based on their frequency. With the seven lowest frequency modes retained, the normal-mode representation has an error of more than 3% in the second flexible mode and an error of more than 0.5% in the second control mode. Convergence

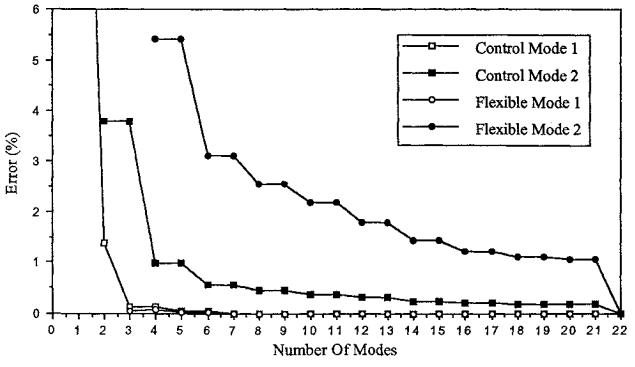

Fig. 5 Error in normal-mode representation closed-loop s-plane pole location with varying number of modes.

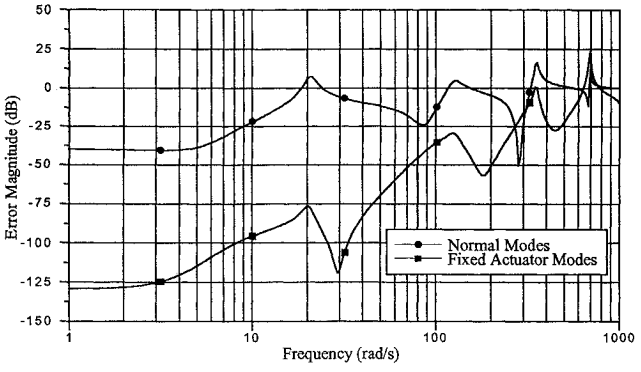

Fig. 6 Command torque to rotation transfer function error: seven-mode ROM.

of the second control mode and the second flexible mode poles is seen to be very slow.

The effects of these errors are more dramatic if we consider the transfer function from torque command to rotation for the two reduced models. Using the relative error measure from Eq. (40), the transfer function errors between the reduced (seven-mode) models and the exact (full-order) model were computed. These are shown in Fig. 6 with the error plotted in decibels. The CB representation low-frequency response is far superior due to the statically complete mode set. As expected,[4] the reduced normal-mode model outperforms the reduced CB model only at isolated zeros of the normal-mode model transfer function. This example demonstrates that the dynamic completeness represented in the proposed controllability measure is effective in mode selection for reduced-order controller design.

To illustrate the use of the controllability measure on structures with unconstrained rigid-body motion, consider the same beam model with only the single torque actuator at the central grid. This permits rigid-body motion in the transverse direction. The controllability measure is computed by projecting out the rigid-body motion from the constrained elastic flexibility matrix in order to compute the constraint mode. Note that in this case the constraint mode is simply a unit rigid-body rotation about grid 11. A very physical interpretation of the controllability is available in this case; only antisymmetric fixed actuator modes will produce net torque at the actuator location, so it is expected that all symmetric modes will be uncontrollable. The controllability measure for the fixed actuator modes is plotted in Fig. 7. Observe that the odd (symmetric) modes are indeed uncontrollable.

As a final example, consider utilization of an observer-based controller. Balas[15] has presented the form of the composite closed-loop system when a reduced-order model (ROM) based controller and observer are used for modal representations. The modal equations are partitioned into *kept* and *residual* blocks and a controller and observer are designed for the ROM utilizing the separation principle. This ignores the residual dynamics, except in the measurements. The

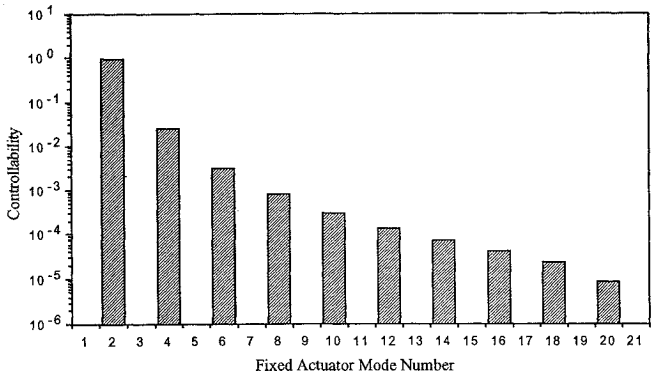

Fig. 7 Unsorted fixed actuator mode controllability: Torque actuator only.

exact closed-loop composite system eigenvalues may be obtained from the matrix

$$\begin{bmatrix} A_k - B_k G & -B_k G & 0 \\ 0 & A_k - LC_k & LC_r \\ -B_r G & -B_r G & A_r \end{bmatrix} \tag{41}$$

where the subscript k refers to "kept" and r to "residual". The matrices (A_i, B_i, C_i) are the corresponding partitions of state-space matrices in modal form, and G and L are the controller and observer gains for the ROM. Assigning pole locations for the ROM plant and observer, Eq. (41) allows assessment of the actual closed-loop pole locations. By using the same control objectives for CB and normal-mode ROMs, the two representations can be compared in observer-based control applications.

For the CB representation, the following definitions are made for the kept and residual partitioning of the CB coordinates:

$$\begin{Bmatrix} z_k \\ \vdots \\ z_r \end{Bmatrix} = \begin{Bmatrix} x_a \\ q_k \\ \vdots \\ q_r \end{Bmatrix} \tag{42}$$

The partitioned form of the CB equation of motion is then given by

$$\begin{bmatrix} \mathcal{M}_{kk} & \mathcal{M}_{kr} \\ \mathcal{M}_{rk} & I_r \end{bmatrix} \begin{Bmatrix} \ddot{z}_k \\ \ddot{z}_r \end{Bmatrix} + \begin{bmatrix} \mathcal{K}_{kk} & 0 \\ 0 & \Lambda_r \end{bmatrix} \begin{Bmatrix} z_k \\ z_r \end{Bmatrix} = \begin{bmatrix} \bar{B}_k \\ 0 \end{bmatrix} u \tag{43}$$

As in the modal case, a controller and observer may be designed for the ROM, ignoring the residual dynamics. Following the development of the matrix in Eq. (41), the exact closed-loop composite system eigenvalues may be obtained from the matrix

$$\begin{bmatrix} \mathcal{A}_{kk} - \mathcal{B}_k G & -\mathcal{B}_k G & \mathcal{A}_{kr} \\ 0 & \mathcal{A}_{kk} - LC_k & LC_r \\ \mathcal{A}_{rk} - \mathcal{B}_r G & -\mathcal{B}_r G & \mathcal{A}_{rr} \end{bmatrix} \tag{44}$$

where

$$\mathcal{A}_{kk} = \begin{bmatrix} 0 & I \\ -N\mathcal{K}_{kk} & 0 \end{bmatrix}, \quad \mathcal{A}_{kr} = \begin{bmatrix} 0 & 0 \\ -N\mathcal{M}_{kr}\Lambda_r^2 & 0 \end{bmatrix},$$

$$\mathcal{A}_{rk} = \begin{bmatrix} 0 & 0 \\ -\mathcal{M}_{rk}N\mathcal{K}_{kk} & 0 \end{bmatrix}$$

$$\mathcal{A}_{rr} = \begin{bmatrix} 0 & I \\ -\mathcal{M}_{rk}N\mathcal{M}_{kr}\Lambda_r^2 & 0 \end{bmatrix}, \quad \mathcal{B}_k = \begin{bmatrix} 0 \\ N\bar{B}_k \end{bmatrix},$$

$$\mathcal{B}_r = \begin{bmatrix} 0 \\ \mathcal{M}_{rk}N\bar{B}_k \end{bmatrix}$$

and $N = (\mathcal{M}_{kk} - \mathcal{M}_{kr}\mathcal{M}_{rk})^{-1}$.

Table 1 CB ROM closed-loop plant and observer pole locations vs actual

Mode	Plant		Observer	
	Desired	Actual	Desired	Actual
Third antisymmetric	$-1 \pm j923.99$	$-51.539 \pm j589.94$	$-1 \pm j923.99$	$-1 \pm j923.99$
Second antisymmetric	$-1 \pm j284.52$	$-1.5417 \pm j283.46$	$-1 \pm j284.52$	$-1 \pm j284.52$
First antisymmetric	$-50 \pm j80$	$-50 \pm j79.9952$	$-10 \pm j80$	$-10 \pm j80$
Control	$-5 \pm j5$	$-5 \pm j5$	$-1 \pm j5$	$-1 \pm j5$

Table 2 Modal ROM closed-loop plant and observer pole locations vs actual

Mode	Plant		Observer	
	Desired	Actual	Desired	Actual
Third antisymmetric	$-1 \pm j592.27$	$-1.065 \pm j592.17$	$-1 \pm j592.27$	$-0.9284 \pm j592.35$
Second antisymmetric	$-1 \pm j283.60$	$-0.9545 \pm j283.71$	$-1 \pm j283.60$	$-1.021 \pm j283.48$
First antisymmetric	$-50 \pm j80$	$-49.268 \pm j71.116$	$-10 \pm j80$	$-10.404 \pm j86.386$
Control	$-5 \pm j5$	$-5.878 \pm j5.2513$	$-1 \pm j5$	$-1.0319 \pm j4.7962$

A ROM for the beam with *torque control only* is now selected for each representation. In the CB ROM, the constraint mode and the first three antisymmetric fixed actuator modes are retained such that 99.9% of the dynamic completeness index is preserved. For the modal ROM, the rigid-body mode and the first three antisymmetric bending modes are selected. Residual modes in both representations are given 1% modal damping for spillover stability. The control objectives are to place the rigid-body mode (control mode) at a frequency of 1 Hz with a damping factor of 0.707 and the first antisymmetric bending mode at 15 Hz with a damping factor of at least 0.5. These two modes will be referred to as the *target modes*. The desired controlled ROM poles and observer poles are shown in Tables 1 and 2 along with the actual (composite system) locations.

The target modes for each representation have identical control objectives, but the two nontarget modes are arbitrarily placed close to their respective open-loop ROM values. Using Eq. (44) the target mode poles for the CB ROM are found to be accurately placed and the corresponding observer poles are placed exactly to significant digits. The nontarget mode poles are not as accurately preserved, but this is acceptable. Using Eq. (41) the target mode poles for the modal ROM are found to be less accurately placed. The modal ROM-based observer pole location errors are also significant. Since the actuation commands are computed from $u = -G\hat{x}$, which depends on the estimated state, the control torques computed by this reduced order controller will have significant error. Clearly, the actuation commands based on the CB ROM will be accurate. In fact, the collocated sensors are measuring physical displacements and velocities directly, so the a-set states need not be estimated at all, and a reduced-order observer could be designed. It is also interesting to note that the control, observation, and dynamic spillover in Eq. (44) all identically vanish if the effective interface mass of the residual modes is zero.

Conclusion

Controllability and observability measures have been derived for a CB representation. These measures facilitate fixed actuator modal ordering and also serve as an index of dynamic completeness for modal truncation. It has thus been shown that use of the CB state space unifies the measures of controllability and dynamic importance. The reduced-order CB models are more accurate for controller design than traditional normal-mode modeling approaches. In conjunction with its widespread use in structural-load analysis and simulation, it has been shown that the CB representation is also an attractive coordinate system choice for control dynamics. It is believed that the CB substructure representation as applied in this investigation will offer significant advantages in future work on decentralized control applications.

Acknowledgments

The authors gratefully acknowledge the support of NASA through the National Space Grant College and Fellowship Program and the Wisconsin Space Grant Consortium and also thank the TRW Space & Technology Group for their continued support.

References

[1]Su, T. J., and Craig, R. R., Jr., "Substructuring Decomposition and Controller Synthesis," AIAA CP-90-1039, 1990.

[2]Young, K. D., "Controlled Component Synthesis: A CSI Approach to Decentralized Control of Structures," *Mechanics and Control of Large Flexible Structures*, edited by J. L. Junkins, AIAA, New York, 1990, pp. 535–564.

[3]Craig, R. R., Jr., and Bampton, M. C. C., "Coupling of Substructures for Dynamic Analysis," *AIAA Journal*, Vol. 6, No. 7, 1968, pp. 1313–1319.

[4]Blelloch, P. A., and Carney, K. S., "Modal Representations in Control/Structure Interaction," *Proceedings of the American Control Conference*, Pittsburgh, PA, 1989, pp. 2802–2807.

[5]Clough, R. W., and Penzien, J., *Dynamics of Structures*, McGraw-Hill, New York, 1975.

[6]Kammer, D. C., and Triller, M. J., "Ranking the Dynamic Importance of Fixed Interface Modes Using a Generalization of Effective Mass," *International Journal of Analytical and Experimental Modal Analysis*, Vol. 9, No. 4, April 1994, pp. 77–98.

[7]Kim, Y., and Junkins, J. L., "Measures of Controllability for Actuator Placement," *Journal of Guidance, Control, and Dynamics*, Vol. 14, No. 5, 1991, pp. 895–902.

[8]Hughes, P. C., and Skelton, R. E., "Controllability and Observability of Linear Matrix-Second Order Systems," *Journal of Applied Mechanics*, Vol. 47, 1980, pp. 415–420.

[9]Hughes P. C., and Skelton, R. E., "Modal Truncation for Flexible Spacecraft," *Journal of Guidance and Control*, Vol. 4, No. 3, 1981, pp. 291–297.

[10]Ohkami, Y., and Likins, P. W., "The Influence of Spacecraft Flexibility on System Controllability and Observability," *Proceedings of the 1974 IFAC*, Malta, USSR, 1974.

[11]Likins, P. W., Ohkami, Y., and Wong, C., "Appendage Modal Coordinate Truncation Criteria in Hybrid Coordinate Dynamic Analysis," *Journal of Spacecraft and Rockets*, Vol. 13, No. 10, 1976, pp. 611–617.

[12]Chen, C. T., *Linear System Theory and Design*, HRW Series in Electrical and Computer Engineering, Holt, Rinehart and Winston, New York, 1984.

[13]Skelton, R. E., *Dynamic Systems Control*, Wiley, New York, 1988.

[14]Kammer, D. C., and Triller, M. J., "Efficient Sensor Placement for On-Orbit Modal Identification of Sequentially Assembled Large Space Structures," *International Journal of Analytical and Experimental Modal Analysis*, Vol. 7, No. 2, 1992, pp. 95–109.

[15]Balas, M. J., "Feedback Control of Flexible Systems," *Institute of Electrical and Electronics Engineers Transactions on Automatic Control*, Vol. 23, 1978, pp. 673–679.

[16]Juang, J. N., and Phan, M., "Robust Controller Designs for Second-Order Dynamic Systems: A Virtual Passive Approach," *Proceedings of the AIAA/ASME/ASCE/AHS/ASC 32nd Structures, Structural Dynamics, and Materials Conference*, AIAA, Washington, DC, 1991, pp. 1796–1805.